



Published in final edited form as:

ACS Appl Mater Interfaces. 2016 July 20; 8(28): 18367–18374. doi:10.1021/acsami.6b04858.

A Bioadhesive Nanoparticle-Hydrogel Hybrid System for Localized Antimicrobial Drug Delivery

Yue Zhang^{a,b}, Jianhua Zhang^{a,c}, Maggie Chen^a, Hua Gong^{a,d}, Soracha Thamphiwatana^{a,b}, Lars Eckmann^e, Weiwei Gao^{a,b}, and Liangfang Zhang^{a,b,*}

^aDepartment of NanoEngineering, University of California, San Diego, La Jolla, CA 92093, USA

^bMoore's Cancer Center, University of California, San Diego, La Jolla, CA 92093, USA

^cDepartment of Polymer Science and Engineering, School of Chemical Engineering and Technology, Tianjin University, Tianjin, 300072, China

^dInstitute of Functional Nano & Soft Materials (FUNSOM), Collaborative Innovation Center of Suzhou Nano Science and Technology, Soochow University, Suzhou, Jiangsu, 215123, China

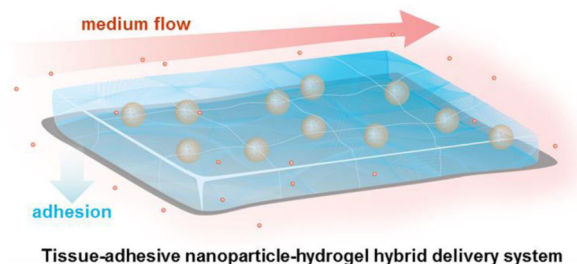
^eDepartment of Medicine, University of California, San Diego, La Jolla, CA 92093, USA

Abstract

Effective antibacterial treatment at the infection site associated with high shear forces remains challenging, owing largely to the lack of durably adhesive and safe delivery platforms that can enable localized antibiotic accumulation against bacterial colonization. Inspired by delivery systems mimicking marine mussels for adhesion, herein, we developed a bioadhesive nanoparticle-hydrogel hybrid (NP-gel) to enhance localized antimicrobial drug delivery. Antibiotics were loaded into polymeric nanoparticles and then embedded into a 3D hydrogel network that confers adhesion to biological surfaces. The combination of two distinct delivery platforms, namely nanoparticles and hydrogel, allows the hydrogel network properties to be independently tailored for adhesion while maintaining controlled and prolonged antibiotic release profile from the nanoparticles. The bioadhesive NP-gel developed here showed superior adhesion and antibiotic retention under high shear stress on a bacterial film, a mammalian cell monolayer, and mouse skin tissue. Under a flow environment, the NP-gel inhibited the formation of an *Escherichia coli* bacterial film. When applied on mouse skin tissue for 7 consecutive days, the NP-gel did not generate any observable skin reaction or toxicity, implying its potential as a safe and effective local delivery platform against microbial infections.

Graphical Abstract

*Corresponding author, Tel: 858-246-0999, zhang@ucsd.edu.



Keywords

Adhesive hydrogel; nanoparticle; catechol; antimicrobial delivery; bacterial infection

1. Introduction

Antibiotics have demonstrated tremendous successes against bacterial infections in the past decades; however, their effectiveness are diminishing due to the rapid emergence of antibiotic-resistant bacterial strains.^{1, 2} To overcome drug resistance, a myriad of nanoparticle-based delivery systems including liposomes, polymeric nanoparticles, dendrimers, and various inorganic nanoparticles have been developed specifically to improve the antimicrobial efficacy of existing antibiotics by altering their pharmacokinetics and biodistribution profiles.^{3, 4} Moreover, nanoparticle technologies have also enabled other novel antibacterial strategies including antibacterial vaccination,^{5, 6, 7} anti-virulence treatment,^{8, 9} and bacterial detection.^{10, 11} Collectively, these research and clinical activities have shown that nanotechnologies, nanoparticles in particular, can play a significant role in combating bacterial infections.

To further enhance the performance and properties of antibacterial nanoparticles, they are increasingly combined with other types of biomaterials to form hybrid complexes for advanced applications. Along this line, loading antibacterial nanoparticles to hydrogels has received much attention and has shown great promise. For instance, nanoparticle-stabilized liposomes, loaded with antimicrobial drugs, have been integrated into a hydrogel matrix. In such hybrid system, the hydrogel not only preserved the structural integrity of the drug-loaded liposomes but also enabled precise control over the viscoelasticity and drug release rate for optimal delivery of drugs.¹² In another example, polymeric nanoparticles wrapped with intact red blood cell membranes, which can absorb and neutralize membrane-damaging toxins (toxin nanosponges), have been loaded into hydrogels to treat local bacterial infections. The hydrogel composition was tailored to effectively retain toxin nanosponges within its matrix without compromising toxin transport for neutralization. This hybrid system retained the nanosponges following subcutaneous injection into mice and effectively neutralized toxins secreted by *Staphylococcus aureus* bacteria and thus significantly reduced skin lesion caused by the toxin-secreted bacteria.¹³ Overall, nanoparticle-hydrogel hybrid (denoted NP-gel) systems judiciously integrate two distinct materials into one formulation with unique physicochemical and biological properties that neither one of the two building blocks can achieve independently.

While various types of NP-gel systems have been developed, it remains highly desirable to develop functional NP-gel formulations that can tolerate high shear forces and thus can work at infection sites involving shear flow of biological fluids. It is not uncommon that bacterial infections occur at sites with high shear forces. For example, bacterial infections within the bloodstream account for a wide range of devastating diseases such as septic shock and meningitis.^{14, 15} In urinary tract, bacterial infections can cause a variety of critical diseases including pyelonephritis, prostatitis, and cystitis.^{16, 17} On corneal surface, bacterial infections are common due to constant exposure of the surface to environmental pathogens; however, the efficiency of delivering antibiotics to cornea has been hampered by the high shear forces from blinking.^{18, 19} In general, the challenges to treat infections under high shear forces are two-fold: first, a high shear force facilitates bacterial adhesion by strengthening the receptor-specific bacterium-host interactions; second, following bacterial colonization, a high shear force prevents effective drug accumulation.^{20, 21}

To address these challenges, herein, we developed a bioadhesive NP-gel system that can effectively adhere to tissue surface for localized delivery of antibiotics to the tissue site under high shear forces (Figure 1A). In the formulation, we used polymeric nanoparticles made from poly(lactic-co-glycolic acid) (PLGA) to encapsulate ciprofloxacin (Cipro), a wide-spectrum antibiotic, for controlled and sustained release. The hydrogel composition was optimized to effectively retain PLGA nanoparticles within its matrix. More importantly, dopamine methacrylamide (DMA), a catechol moiety responsible for marine mussel adhesion to a variety of surfaces, was integrated into the hydrogel network through a copolymerization process.^{22, 23} Similar biomimetic chemistry for adhesiveness has been demonstrated in various synthetic hydrogels aimed for a variety of adhesive applications.^{24, 25, 26, 27} We hypothesize that with a strong adhesive force, the tissue-adhesive NP-gel system can withstand physiologically relevant shear stresses without detaching from biological surfaces, allowing for controlled and localized antibiotic release for effective bioactivity. In the study, superior adhesion and antibiotic retention under high shear stresses were verified on three representative biological subjects, including a bacterial film, a mammalian cell monolayer, and mouse skin tissue. Under flow conditions, the Cipro-loaded NP-gel showed great effectiveness in inhibiting the formation of *Escherichia coli* (*E. coli*) biofilm. Furthermore, when applied topically on mouse skin, the NP-gel did not generate any observable skin reaction or toxicity within a 7-day treatment period, implying its potential as a safe and effective local delivery platform against bacterial infections.

2. Experimental Section

Synthesis of dopamine methacrylamide (DMA)

Dopamine hydrochloride, methacrylic acid *N*-hydroxysuccinimide ester (MNHS), triethylamine (TEA), ethyl acetate, tetrahydrofuran (THF), and *N,N*-Dimethylformamide-*d*₇ (d-DMF) were purchased from Sigma-Aldrich (St. Louis, MO, USA). DMA was synthesized by conjugating MNHS with dopamine in THF with the presence of TEA. Specifically, dopamine (758.4 mg, 4 mmol) and MNHS (489.1 mg, 2.67 mmol) were dissolved together in THF (9.5 mL), and TEA (0.5 mL) was added to the mixture solution. The mixture was stirred at room temperature and the reaction was allowed to proceed for 24

hrs. The THF was then evaporated. To the remaining powder in the vial, 5 mL DI water was added and stirred, and the pH of the solution was adjusted to 5. For purification, 5 mL ethyl acetate was added and the mixture was vigorously vortexed to extract DMA. The extraction process was repeated three times and the collected ethyl acetate solutions were combined and then evaporated. The final product was collected as pale white powder. The product was dissolved with d-DMF and the ¹HNMR spectra were obtained on a Varian Inova-500M instrument (Varian Inc., Palo Alto, CA, USA). To confirm the conjugated product, chromatographic analysis was performed on a Perkin Elmer Flexar High Performance Liquid Chromatography (HPLC, series 200) consisting of a Brownlee SPP C18 column (100 mm length × 4.6 mm diameter column filled with 2.7 μm diameter beads). The mobile phase was acetonitrile: water (50:50, v:v) at a flow rate of 1.0 mL/min at 30°C. For each analysis, 20 μL of the sample was injected and detected at a wavelength of 240 nm.

Synthesis of polymeric nanoparticles

Poly (lactic-co-glycolic acid) (PLGA, 50:50, inherent viscosity = 0.67 dl/g) was purchased from LACTEL Absorbable Polymers (Birmingham, AL, USA). The surfactant F-127 was purchased from Sigma (St. Louis, MO, USA). Ciprofloxacin (HCl salt, Cipro) was purchased from Fluka (Milwaukee, WI, USA). Fluorescent dye benzoxazolium, 3-octadecyl-2-[3-(3-octadecyl-2(3H)-benzoxazolylidene)-1-propenyl]-, perchlorate (DiO, excitation/emission = 484/501 nm) was purchased from ThermoFisher Scientific (Carlsbad, CA, USA). Briefly, 20 μL of 20 mg/mL Cipro solution was emulsified in 0.5 mL chloroform containing 5 mg/mL PLGA and 5 mg/mL Pluronic F-127 with a probe sonicator (Fisher Scientific). The sonication last 1 min with intermittence of 1 s and a power of 12 W at room temperature. Then the emulsion was added to 10 mL of a 7% (w/v) Pluronic F-127 aqueous solution and sonicated for another 2 min. The emulsion was stirred overnight to allow chloroform to evaporate. The resulting nanoparticle suspension was then centrifuged at 16,100 ×g for 5 mins to collect nanoparticles, which were subsequently washed with distilled water and lyophilized for future use. DiO-loaded nanoparticles were prepared using a similar procedure by replacing Cipro with the dye. The size and size distribution of nanoparticles were measured with dynamic light scattering (DLS) (Zetasizer Nano, Malvern, UK). The rheological analysis was carried out at 37 °C using a strain-controlled AR-G2 rheometer with 22 mm diameter parallel-plate geometry (TA Instruments Inc., New Castle, DE). Oscillatory rheological measurements were performed in the linear viscoelastic regime. The strain was kept at 0.1% and a dynamic frequency sweep from 0.1 to 10 rad/s was conducted to measure the storage modulus G' and loss modulus G'' .

Preparation of nanoparticle-hydrogel hybrid (NP-gel) formulation

Acrylamide (used as monomer), poly(ethylene glycol) dimethacrylate (PEGDMA, used as cross-linker), and poly(vinyl alcohol) (PVA) were purchased from Sigma-Aldrich (St. Louis, MO, USA). Lithium phenyl-2,4,6-trimethylbenzoylphosphinate (LAP, used as photo-initiator) was synthesized by following a published protocol.^{28, 29} To prepare NP-gel, the final concentrations of acrylamide, LAP, and nanoparticles were kept constant at 100, 3, and 2 mg/mL, respectively, while DMA and PEGDMA concentrations were varied in the range of 0 – 5 mg/mL. For polymerization, all samples were irradiated by using an UV lamp (Black Ray® UVL-56, UVP Ltd, Upland, CA, USA) at 365 nm with a power of 4 W for 3

min. To measure nanoparticle release from the hydrogel, DiO-labeled nanoparticles were used to prepare the NP-gel at different PEGDMA concentrations. Then 0.5 mL NP-gel was submerged into 50 mL $1\times$ PBS. The mixture was incubated at 37°C for 24 hrs and the DiO signal from the supernatant was measured with a fluorescent spectrophotometer (Infinite M200, TECAN, Switzerland). To test the adhesion property of the NP-gel, a PVA film was made by first mixing 1 g glutaraldehyde with 10 mL 10 wt% PVA solution followed by drying overnight at 70°C.³⁰ NP-gels (20 μ L) formulated with different DMA concentrations were mixed with 2 μ L periodate (1 mg/mL) and applied onto the PVA film. Then the film was placed in the center of a cylindrical flow channel with a diameter of 5.85 mm. Deionized (DI) water flew through the channel and the shear stress (τ) imposed on the NP-gel sample was calculated from a modified Darcy-weisbach equation: $\tau = C_f \rho V^2/2$, where C_f is the coefficient of friction (0.0015), ρ is the density of water (1 g/cm³), and V is the fluid velocity (m/s).³¹ To study NP-gel morphology, it was first lyophilized (overnight, 2.5 L Labconco benchtop freeze system) and the flakes of the NP-gel were then placed on a silicon wafer. The samples were coated with iridium and then examined with scanning electron microscope (SEM, FEI Philips XL30 ESEM).

NP-gel adhesion to biological subjects

To prepare bacterial biofilms, *E. coli* bacteria (K12, Strain SMG 123, ATCC PTA-7555, Manassas, VA, USA) were grown in Luria Broth (LB) media (Thermo Fisher Scientific) at 37°C. Sterilized coverslips were submerged into the medium (containing 2×10^7 CFU/mL bacteria) and cultured for 24 hrs. The biofilm formation was confirmed with 0.1% crystal violet stain.¹⁶ To prepare mammalian cell monolayer, HEK293T cells (ATCC, Manassas, VA, USA) was cultured in high glucose DMEM cell culture medium supplemented with 10% fetal bovine serum and 1% penicillin/streptomycin under 37°C with 5% carbon dioxide. Cells were grown on a 1 cm \times 1 cm cover slip until they reached confluence (approximately 1×10^5 cells/cm²). To prepare mouse skin sample, the skin of ICR mice (Charles Rivers Laboratory, Wilmington, MA, USA) was shaved and cut into 25 cm \times 40 cm pieces. To test NP-gel adhesion, bacterial film and HEK 293T cell monolayer were fixed with 10% formalin for 30 min at room temperature. The bacterial film was stained with propidium iodide (PI) and the cell monolayer was stained with DAPI (1 mg/mL). Then, 20 μ L NP-gel (loaded with DiO-labeled nanoparticles) was applied onto each sample. The sample was then placed inside a flow channel and subject to a shear stress of 3.2 Pa for 5 min. After the flow, the samples were examined under Olympus FV1000 Confocal Microscopy. For peeling test, 100 μ L of NP-gel was sandwiched between two pieces of mouse skin. The sample was pressed under a constant pressure of \sim 50 Pa for 5 min to ensure close contact between the hydrogel and the skin. The peel force was measured using Testometric AX M350-10KN materials testing machine (Testometric Company, Germany) operated at 25 mm/s. In the present study, the adhesion property was activated by adding periodate; NP-gels without addition of periodate were used as controls. Statistical analysis was performed with GraphPad Prism using an unpaired two-tailed *t*-test.

Ciprofloxacin (Cipro) loading yield and release measurements

To measure Cipro loading yield, nanoparticles were dissolved with dimethyl sulphoxide (DMSO), followed by adding 10 volumes of DI water. Polymer precipitates were removed

by centrifugation. The solution was measured for Cipro fluorescence intensity (excitation/emission = 270/440 nm).^{32, 33} A standard calibration curve was made by measuring serial dilutions of Cipro solution (0 – 10 mg/mL) and the Cipro concentration was determined by comparing with the standard calibration curve. To study Cipro release from NP-gel, 0.5 mL NP-gel was placed inside a dialyzer (Harvard Apparatus, Holliston, MA, USA) and the dialysis membrane with a pore size of 100 nm (Isopore Membrane filters, Millipore, Billerica, MA, USA) was used. The dialyzer was submerged into 100 mL 1× PBS and stirred at 37°C. At predetermined time intervals, 1.0 mL of the solution was taken and the same volume of PBS was added. Cipro concentration was determined also by fluorescence measurement.

Antibiofilm efficacy of Cipro-loaded NP-gel

To determine the local anti-bacterial activity of NP-gel, sterilized polycarbonate membranes (Whatman, nucleopore track-etch membrane, 25 mm diameter, 100 nm pore size) were inoculated with 10 μ L *E. coli* DH5 α (OD_{600} = 0.005, corresponding to a bacterial concentration of 5×10^6 CFU/mL)⁶. The membrane was then placed into the wells of a 24-well plate. On top of the membrane, 100 μ L NP-gel loaded with Cipro at a concentration of 0.625 μ g/mL was applied and then 2 mL culture medium was added. In parallel, membranes added with PBS, hydrogel only (without nanoparticle or drug), free Cipro, and Cipro-loaded nanoparticles (without hydrogel) were used as control groups. To simulate the decrease of drug concentration under flow conditions, the medium was diluted half with fresh medium at 0, 3, 6, 9, and 12 hr time points. At 15 hr, the membranes together with the medium were transferred to microtubes and vortexed vigorously. The suspension was then serially diluted with PBS and inoculated onto LB agar plate for bacterial count enumeration. Statistical analysis was performed with GraphPad Prism using an unpaired two-tailed t-test.

Skin toxicity evaluation of NP-gel

ICR mice were shaved on the back 24 hrs before the toxicity test. The NP-gel was administrated onto the shaved area once a day in a period of 7 days. The mice administrated with PBS served as a control group. After the final treatment, all the mice were sacrificed and the treated areas were collected with 8 mm biopsy punch for histological examination. To fix the tissue, the skin samples were immersed into 10% formalin for 18 hrs and then embedded in paraffin. Hematoxylin and eosin (H&E) staining and terminal deoxynucleotidyl transferase-mediated deoxyuridine triphosphate nick-end labeling (TUNEL) assay (Boehringer Mannheim, Indianapolis, IN, USA) were used to evaluate the cellular morphology change and apoptosis, respectively. Tissue slices were imaged with Hamamatsu Nanosommer 2.0 HT and the images were processed with NDP Viewer software.

3. Results and discussion

In the study, we first synthesized dopamine methacrylamide (DMA) by directly conjugating dopamine with methacrylate *N*-hydroxysuccinimide ester (MNHS) in tetrahydrofuran (THF) with the presence of triethylamine (TEA). Upon purification, the molecular structure of the product was analyzed with ¹H-NMR. The spectrum shows the characteristic resonance signals of catechol hydroxyl groups (8.85 ppm), phenyl protons (6.7 and 6.5 ppm),

methylene protons (3.4 and 2.6 ppm), and alkenyl hydrogens (5.7 and 5.3 ppm), which are all consistent with those of DMA (Figure 1 B).^{24, 26} Further analysis using high-performance liquid chromatography (HPLC) shows that the product has a single peak with a longer elution time of 1 min compared to 0.8 min of dopamine precursor, indicating successful conjugation and purification (Figure 1C).

Following the synthesis of DMA, we proceeded to prepare the bioadhesive NP-gel. The preparation was divided into two steps. In the first step, the PLGA nanoparticles encapsulating Cipro were prepared by a double emulsion solvent evaporation technique and using Pluronic F-127 as surfactant. Then the first emulsion was transferred to 10 mL 7% (w/v) F-127 aqueous solution. The double emulsion was stirred overnight to evaporate the remaining chloroform, resulting in nanoparticles with an average diameter of 151.3 ± 5.5 nm and a PDI value of 0.28 ± 0.04 (Figure 1D). In the second step, the nanoparticles were mixed with DMA (a monomer and adhesive moiety), acrylamide (AAM, a monomer), poly(ethylene glycol) dimethacrylate (PEGDMA, a crosslinker), and lithium phenyl-2,4,6-trimethylbenzoylphosphinate (LAP, the photo-initiator). The final concentrations of AAM, LAP, and nanoparticles were kept constant at 100, 3, and 2 mg/mL, respectively, while DMA and PEGDMA concentrations were varied in the range of 0 – 5 mg/mL. Hydrogelation was achieved by irradiating the sample under UV light with a wavelength of 365 nm for 3 min at room temperature.

The hydrogel formulation was first optimized for effective nanoparticle retention. Specifically, we labeled the PLGA nanoparticles with 3,3'-Dioctadecyloxacarbocyanine perchlorate (DiO, excitation/emission=484 nm/501 nm), a hydrophobic fluorophore with negligible leakage from PLGA nanoparticles at the experimental conditions.³⁴ Then we fixed the concentration of PLGA nanoparticles, AAM, DMA and LAP at 2 mg/mL (PLGA content), 100 mg/mL, 5 mg/mL and 3 mg/mL, respectively, but varied PEGDMA concentrations and correspondingly measured nanoparticle release profiles from the hydrogel. As shown in Figure 1D, the accumulated release of nanoparticles over 24 hrs decreased sharply from 92.3% at 1 mg/mL PEGDMA concentration to 9.0% at 5 mg/mL, suggesting that 5 mg/mL crosslinker concentration was sufficient to retain the nanoparticles in the hydrogel matrix. This PEGDMA concentration was then used to prepare NP-gels for the subsequent studies.

We next optimized DMA concentration in the NP-gel formulation by evaluating its adhesive strength on a polyvinyl alcohol (PVA) film, which simulates biological surfaces because of its high density of terminal hydroxyl groups.^{35, 36} In the study, the concentrations of PLGA nanoparticles, AAM, PEGDMA, and LAP were kept constant, but DMA concentration was varied from 0 to 5 mg/mL. The adhesion of the corresponding NP-gels was examined in a cylindrical flow channel, where the shear stress was controlled by flow rate. The adhesion was activated by adding periodate, an oxidant that has been used to oxidize catechol-containing hydrogels in vivo for islet implantation.^{25, 37} As shown in Figure 1E, without DMA, the shear stress required to completely wash away the NP-gel was 0.23 Pa. However, at 5 mg/mL DMA concentration, the needed shear stress increased to 6.7 Pa, a value much higher than that generated by physiological blood flow.³⁸ We therefore chose 5 mg/mL DMA concentration to prepare bioadhesive NP-gels for the following studies.

The NP-gel was further analyzed with dynamic rheological measurements of the storage modulus (G') and the loss modulus (G'') as a function of frequency (Figure 1 G). In the study, G' exceeded G'' over the entire frequency range, a clear viscoelastic behavior indicating the formation of a hydrogel network. In addition, G' and G'' values measured from NP-gel were generally close to those measured from the empty hydrogel (without PLGA nanoparticles), suggesting a minor effect of the loaded PLGA nanoparticles on the hydrogel rheological characteristics. Following the formulation optimization, the NP-gel sample was lyophilized and the sample appeared as white powders. Flakes from the sample were examined for morphology with scanning electron microscopy (SEM) (Figure 1H). The NP-gel sample showed characteristic porous sponge-like structures with some irregular lamellar feature (Figure 1I). At a higher magnification, nanoparticles with a diameter of approximately 150 nm embedded within the hydrogel network were observed (Figure 1I, inset).

To evaluate the cell- and tissue-adhesive properties of the resulting NP-gel and its ability to retain the embedded nanoparticles under flow conditions, we prepared three representative biological surfaces, namely a bacterial film, a mammalian cell monolayer, and shaved mouse skin tissue. The bacterial film was formed on a glass coverslip by immersing it into *E. coli* bacterial suspension and culturing together with the bacteria. The bacterial film was stained with Propidium iodide (red) and the NP-gel containing DiO-labeled nanoparticles (green) was applied on top of the film. The sample was placed inside the cylindrical flow channel and subjected to a shear stress of 3 Pa for 10 min. This shear stress value was chosen because it is comparable to that of physiological blood flow.^{25, 38} After the flow treatment, DiO-labeled nanoparticles remained clearly visible under the fluorescence microscope (Figure 2A). However, when the non-adhesive NP-gel (negative control, without addition of periodate) was placed under the same flow condition, little fluorescence from the nanoparticles was detected (Figure 2B). Further quantification of the nanoparticle retention showed that nearly 100% of the nanoparticles in the bioadhesive NP-gel remained on the bacterial film after the flow, whereas only about 8% of the nanoparticles in the non-adhesive NP-gel were retained in the hydrogel (Figure 2C). Similarly, under the same flow condition, significantly more nanoparticles in the bioadhesive NP-gel (Figure 2D, green color) were retained on a HEK 293T cell monolayer cultured on a glass coverslip as compared to those in the non-adhesive NP-gel (Figure 2E). Fluorescence intensity emitted from the retained nanoparticles showed that nearly 100% of the nanoparticles remained on the HEK 293T cell monolayer when the adhesive NP-gel was used, contrasting sharply to merely ~3% retention for the non-adhesive NP-gel (Figure 2F). On mouse skin, stronger adhesion property of the adhesive NP-gel was also observed. The adhesive NP-gel sample applied on the skin surface was intact after the flow (Figure 2G), whereas the non-adhesive NP-gel was readily washed off by the flow. In a standard peeling test where 100 μ L of adhesive NP-gel was sandwiched between two pieces of mouse skin, a peel force of ~0.3 N was needed to peel one skin specimen off from the other. In contrast, only ~0.03 N peel force was needed to separate the two skin specimen when the non-adhesive NP-gel was used.

After having demonstrated the enhanced adhesion properties of the NP-gel on biological surfaces, we proceeded to evaluate its local antibacterial delivery effectiveness, especially under flow conditions. We first examined Cipro release profile from the NP-gel and

compared it with that from blank hydrogel (without nanoparticles) loaded with free Cipro molecules (Figure 3A). The NP-gel showed a gradual release profile, where 48.5%, 68.3%, and 88.2% of loaded Cipro molecules were released at 24, 48, and 72 hrs, respectively. In contrast, free Cipro showed a burst release profile from the blank hydrogel, releasing 94.4% Cipro molecules in the first 12 hrs, followed by a slow release of 98.4% at 72 hrs. This comparison of drug release profiles clearly demonstrates the advantage of NP-gel in enabling controlled and sustained drug release kinetics. Notably, for future applications, the duration of gel adhesion may need to match the time span for releasing the majority of antibiotics as the gel without antibiotics could potentially encourage bacterial colonization. Such temporal control can be achieved by either tailoring the degradation rate of the hydrogel³⁹ or tuning antibiotic release rate of the nanoparticles.⁴⁰

To investigate the *in vitro* antibacterial efficacy of the Cipro-loaded NP-gel, we first inoculated 5×10^4 CFU *E. coli* DH5 α bacteria onto porous polycarbonate membranes placed inside the wells of a 24-well plate. Then onto the top of the membrane, 100 μ L Cipro-loaded NP-gel was applied and 2 mL culture medium was supplemented. Wells added with blank gel (without nanoparticles or Cipro), free Cipro, Cipro-loaded nanoparticles (without hydrogel) were used as control groups. In all wells, Cipro, if present, was kept at the same concentration of 0.63 mg/mL. To simulate the decrease of drug concentration under flow conditions, half of the medium (1 mL) was removed at the time points of 0, 3, 6, 9, and 12 hrs and each well was replenished with the same amount of fresh medium. As shown in Figure 3B, 15 hrs after the initial bacterial inoculation, samples treated with all control groups developed visible bacterial films with similar sizes on the polycarbonate membrane. However, there was no visible colony formation on the polycarbonate membrane treated with Cipro-loaded NP-gel, indicating its high antibacterial efficacy. To further quantify the bacterial growth, we then disaggregated the bacterial film on each membrane for bacterial enumeration. As shown in Figure 3C, bacteria in all control groups multiplied approximately 4-order of magnitude from the initial 5×10^4 CFU/membrane, while bacteria number decreased to about 1×10^4 CFU for the group treated with Cipro-loaded NP-gel.

Lastly, we examined the skin toxicity of the NP-gel by using a mouse skin model as described before. The mouse back skin was shaved 24 hrs before the experiment to allow for full recovery from possible disturbance to the stratum corneum by the shaving process. Then the tissue-adhesive NP-gel was topically applied to the shaved area once a day for 7 days. The mice treated with PBS served as a control group. After the 7-day treatment, the skin morphology was observed. As shown in Figure 4A and B, the structure of the skin treated with NP-gel was similar to that of PBS group. There was no visible indication of toxicity such as erythema and edema. Following that, the skin biopsy was collected and stained with hematoxylin and eosin (H&E), (Figure 4C and D) the NP-gel treated skin showed similar structure as the PBS treated group; both of them showed a clean and clear layer of healthy epidermal cells on the top of dermis layer. To further study the NP-gel toxicity, the skin samples were also stained with a terminal deoxynucleotidyl transferase-mediated deoxyuridine triphosphate nick-end labeling (TUNEL) assay. Compared with PBS treated group, there was no obvious increase of apoptotic cells in the NP-gel treated skin. (Figure 4E and F). Overall, the toxicity results suggest that NP-gel is safe for a seven-day topical administration.

4. Conclusions

In summary, a bioadhesive nanoparticle-hydrogel hybrid (NP-gel) system was developed to enhance localized antimicrobial drug delivery, especially under high shear force conditions. In the design, antibiotics were loaded into polymeric nanoparticles and then embedded into a tissue-adhesive hydrogel. The hybrid system showed superior adhesion and antibiotic retention under high shear stress on biological surfaces including a bacterial film, a mammalian cell monolayer, and mouse skin tissue. Under a flow environment in vitro, the NP-gel inhibited effectively the formation of *E. coli* bacterial film. When test on mouse skin, the NP-gel did not generate any observable skin reaction or toxicity within a 7-day treatment period. Notably, the bioadhesive NP-gel developed here can be potentially applied to treat various other diseases by choosing appropriate therapeutic agents and nanoparticle cargos. The adhesion property and viscoelasticity of the NP-gel can be tailored to match the need of shear stresses under specific physiological conditions. Overall, the biologically adhesive NP-gel delivery system that uses adhesive force to overcome high shear forces holds significant potential for prolonged, safe and effective localized delivery of various therapeutic agents.

Acknowledgments

This work is supported by the Defense Threat Reduction Agency Joint Science and Technology Office for Chemical and Biological Defense under Grant Number HDTRA1-16-1-0013 and the National Institutes of Health under Award Number R21AI119459.

References

1. Fauci AS, Morens DM. The Perpetual Challenge of Infectious Diseases. *N. Engl. J. Med.* 2012; 366:454–461. [PubMed: 22296079]
2. Farmer PE. Chronic Infectious Disease and the Future of Health Care Delivery. *N. Engl. J. Med.* 2013; 369:2424–2436. [PubMed: 24350951]
3. Zhang L, Pornpattananangkul D, Hu CMJ, Huang CM. Development of Nanoparticles for Antimicrobial Drug Delivery. *Curr. Med. Chem.* 2010; 17:585–594. [PubMed: 20015030]
4. Gao W, Thamphiwatana S, Angsantikul P, Zhang L. Nanoparticle Approaches against Bacterial Infections. *Wiley Interdiscip. Rev. Nanomed. Nanobiotechnol.* 2014; 6:532–547. [PubMed: 25044325]
5. Hu C-MJ, Fang RH, Luk BT, Zhang L. Nanoparticle-Detained Toxins for Safe and Effective Vaccination. *Nat. Nanotechnol.* 2013; 8:933–938. [PubMed: 24292514]
6. Gao W, Fang RH, Thamphiwatana S, Luk BT, Li J, Angsantikul P, Zhang Q, Hu C-MJ, Zhang L. Modulating Antibacterial Immunity Via Bacterial Membrane-Coated Nanoparticles. *Nano Lett.* 2015; 15:1403–1409. [PubMed: 25615236]
7. Wang F, Fang R, Luk B, Hu C-M, Thamphiwatana S, Dehaini D, Angsantikul P, Kroll A, Pang Z, Gao W, Lu W, Zhang L. Nanoparticle-Based Anti-Virulence Vaccine for the Management of Methicillin-Resistant *Staphylococcus Aureus* Skin Infection. *Adv. Funct. Mater.* 2016; 26:1628–1635. [PubMed: 27325913]
8. Hu C-MJ, Fang RH, Copp J, Luk BT, Zhang L. A Biomimetic Nanosponge That Absorbs Pore-Forming Toxins. *Nat. Nanotechnol.* 2013; 8:336–340. [PubMed: 23584215]
9. Gou M, Qu X, Zhu W, Xiang M, Yang J, Zhang K, Wei Y, Chen S. Bio-Inspired Detoxification Using 3d-Printed Hydrogel Nanocomposites. *Nat. Commun.* 2014; 5 Article number 3774.
10. Chung HJ, Castro CM, Im H, Lee H, Weissleder R. A Magneto-DNA Nanoparticle System for Rapid Detection and Phenotyping of Bacteria. *Nat. Nanotechnol.* 2013; 8:369–375. [PubMed: 23644570]

11. Mezger A, Fock J, Antunes P, Osterberg FW, Boisen A, Nilsson M, Hansen MF, Ahlford A, Donolato M. Scalable DNA-Based Magnetic Nanoparticle Agglutination Assay for Bacterial Detection in Patient Samples. *ACS Nano*. 2015; 9:7374–7382. [PubMed: 26166357]
12. Gao W, Vecchio D, Li J, Zhu J, Zhang Q, Fu V, Li J, Thamphiwatana S, Lu D, Zhang L. Hydrogel Containing Nanoparticle-Stabilized Liposomes for Topical Antimicrobial Delivery. *ACS Nano*. 2014; 8:2900–2907. [PubMed: 24483239]
13. Wang F, Gao W, Thamphiwatana S, Luk BT, Angsantikul P, Zhang Q, Hu C-MJ, Fang RH, Copp JA, Pornpattananangkul D, Lu W, Zhang L. Hydrogel Retaining Toxin-Absorbing Nanosponges for Local Treatment of Methicillin-Resistant Staphylococcus Aureus Infection. *Adv. Mater.* 2015; 27:3437–3443. [PubMed: 25931231]
14. Mikaty G, Soyer M, Mairey E, Henry N, Dyer D, Forest KT, Morand P, Guadagnini S, Prevost MC, Nassif X, Dumenil G. Extracellular Bacterial Pathogen Induces Host Cell Surface Reorganization to Resist Shear Stress. *PLoS Pathog.* 2009; 5 article number e1000314.
15. Garciarena CD, McHale TM, Watkin RL, Kerrigan SW. Coordinated Molecular Cross-Talk between Staphylococcus Aureus, Endothelial Cells and Platelets in Bloodstream Infection. *Pathogens*. 2015; 4:869–882. [PubMed: 26690226]
16. Cusumano CK, Pinkner JS, Han Z, Greene SE, Ford BA, Crowley JR, Henderson JP, Janetka JW, Hultgren SJ. Treatment and Prevention of Urinary Tract Infection with Orally Active FimH Inhibitors. *Sci. Transl. Med.* 2011; 3 article number 109ra115.
17. Nielubowicz GR, Mobley HLT. Host-Pathogen Interactions in Urinary Tract Infection. *Nat. Rev. Urol.* 2010; 7:430–441. [PubMed: 20647992]
18. Alarcon I, Kwan L, Yu C, Evans DJ, Fleiszig SMJ. Role of the Corneal Epithelial Basement Membrane in Ocular Defense against Pseudomonas Aeruginosa. *Infect. Immun.* 2009; 77:3264–3271. [PubMed: 19506010]
19. Rivers HM, Chaudhuri SR, Shah JC, Mittal S. A New Vision for the Eye: Unmet Ocular Drug Delivery Needs. *Pharm. Res.* 2015; 32:2814–2823. [PubMed: 26055402]
20. Thomas WE, Trintchina E, Forero M, Vogel V, Sokurenko EV. Bacterial Adhesion to Target Cells Enhanced by Shear Force. *Cell*. 2002; 109:913–923. [PubMed: 12110187]
21. Nilsson LM, Thomas WE, Sokurenko EV, Vogel V. Elevated Shear Stress Protects Escherichia Coli Cells Adhering to Surfaces Via Catch Bonds from Detachment by Soluble Inhibitors. *Appl. Environ. Microbiol.* 2006; 72:3005–3010. [PubMed: 16598008]
22. Lee H, Dellatore SM, Miller WM, Messersmith PB. Mussel-Inspired Surface Chemistry for Multifunctional Coatings. *Science*. 2007; 318:426–430. [PubMed: 17947576]
23. Lee H, Scherer NF, Messersmith PB. Single-Molecule Mechanics of Mussel Adhesion. *Proc. Natl. Acad. Sci. U. S. A.* 2006; 103:12999–13003. [PubMed: 16920796]
24. Lee H, Lee BP, Messersmith PB. A Reversible Wet/Dry Adhesive Inspired by Mussels and Geckos. *Nature*. 2007; 448:338–341. [PubMed: 17637666]
25. Kastrop CJ, Nahrendorf M, Figueiredo JL, Lee H, Kambhampati S, Lee T, Cho S-W, Gorbatov R, Iwamoto Y, Dang TT, Dutta P, Yeon JH, Cheng H, Pritchard CD, Vegas AJ, Siegel CD, MacDougall S, Okonkwo M, Anh T, Stone JR, Coury AJ, Weissleder R, Langer R, Anderson DG. Painting Blood Vessels and Atherosclerotic Plaques with an Adhesive Drug Depot. *Proc. Natl. Acad. Sci. U. S. A.* 2012; 109:21444–21449. [PubMed: 23236189]
26. Skelton S, Bostwick M, O'Connor K, Konst S, Casey S, Lee BP. Biomimetic Adhesive Containing Nanocomposite Hydrogel with Enhanced Materials Properties. *Soft Matter*. 2013; 9:3825–3833.
27. Lee BP, Konst S. Novel Hydrogel Actuator Inspired by Reversible Mussel Adhesive Protein Chemistry. *Adv. Mater.* 2014; 26:3415–3419. [PubMed: 24596273]
28. Fairbanks BD, Schwartz MP, Bowman CN, Anseth KS. Photoinitiated Polymerization of Peg-Diacrylate with Lithium Phenyl-2,4,6-Trimethylbenzoylphosphinate: Polymerization Rate and Cytocompatibility. *Biomaterials*. 2009; 30:6702–6707. [PubMed: 19783300]
29. Ma Y, Thiele J, Abdelmohsen L, Xu J, Huck WTS. Biocompatible Macro-Initiators Controlling Radical Retention in Microfluidic on-Chip Photopolymerization of Water-in-Oil Emulsions. *Chem. Commun.* 2014; 50:112–114.
30. Otsuka E, Suzuki A. A Simple Method to Obtain a Swollen Pva Gel Crosslinked by Hydrogen Bonds. *J. Appl. Polym. Sci.* 2009; 114:10–16.

31. Dosunmu IT, Shah SN. Pressure Drop Predictions for Laminar Pipe Flow of Carreau and Modified Power Law Fluids. *Can. J. Chem. Eng.* 2015; 93:929–934.
32. Yang R, Fu Y, Li LD, Liu JM. Medium Effects on Fluorescence of Ciprofloxacin Hydrochloride. *Spectrochim. Acta, Part A.* 2003; 59:2723–2732.
33. Sowinski KM, Kays MB. Determination of Ciprofloxacin Concentrations in Human Serum and Urine by HPLC with Ultraviolet and Fluorescence Detection. *J. Clin. Pharm. Ther.* 2004; 29:381–387. [PubMed: 15271106]
34. Gaumet M, Gurny R, Delie F. Fluorescent Biodegradable Plga Particles with Narrow Size Distributions: Preparation by Means of Selective Centrifugation. *Int. J. Pharm.* 2007; 342:222–230. [PubMed: 17574353]
35. Chiellini E, Corti A, D'Antone S, Solaro R. Biodegradation of Poly (Vinyl Alcohol) Based Materials. *Prog. Polym. Sci.* 2003; 28:963–1014.
36. Baker MI, Walsh SP, Schwartz Z, Boyan BD. A Review of Polyvinyl Alcohol and Its Uses in Cartilage and Orthopedic Applications. *J. Biomed. Mater. Res. Part B.* 2012; 100B:1451–1457.
37. Brubaker CE, Kissler H, Wang L-J, Kaufman DB, Messersmith PB. Biological Performance of Mussel-Inspired Adhesive in Extrahepatic Islet Transplantation. *Biomaterials.* 2010; 31:420–427. [PubMed: 19811819]
38. Gnasso A, Carallo C, Irace C, Spagnuolo V, DeNovara G, Mattioli PL, Pujia A. Association between Intima-Media Thickness and Wall Shear Stress in Common Carotid Arteries in Healthy Male Subjects. *Circulation.* 1996; 94:3257–3262. [PubMed: 8989138]
39. Hoffman AS. Hydrogels for Biomedical Applications. *Adv. Drug. Del. Rev.* 2012; 64:18–23.
40. Kamaly N, Yameen B, Wu J, Farokhzad OC. Degradable Controlled-Release Polymers and Polymeric Nanoparticles: Mechanisms of Controlling Drug Release. *Chem. Rev.* 2016; 116:2602–2663. [PubMed: 26854975]

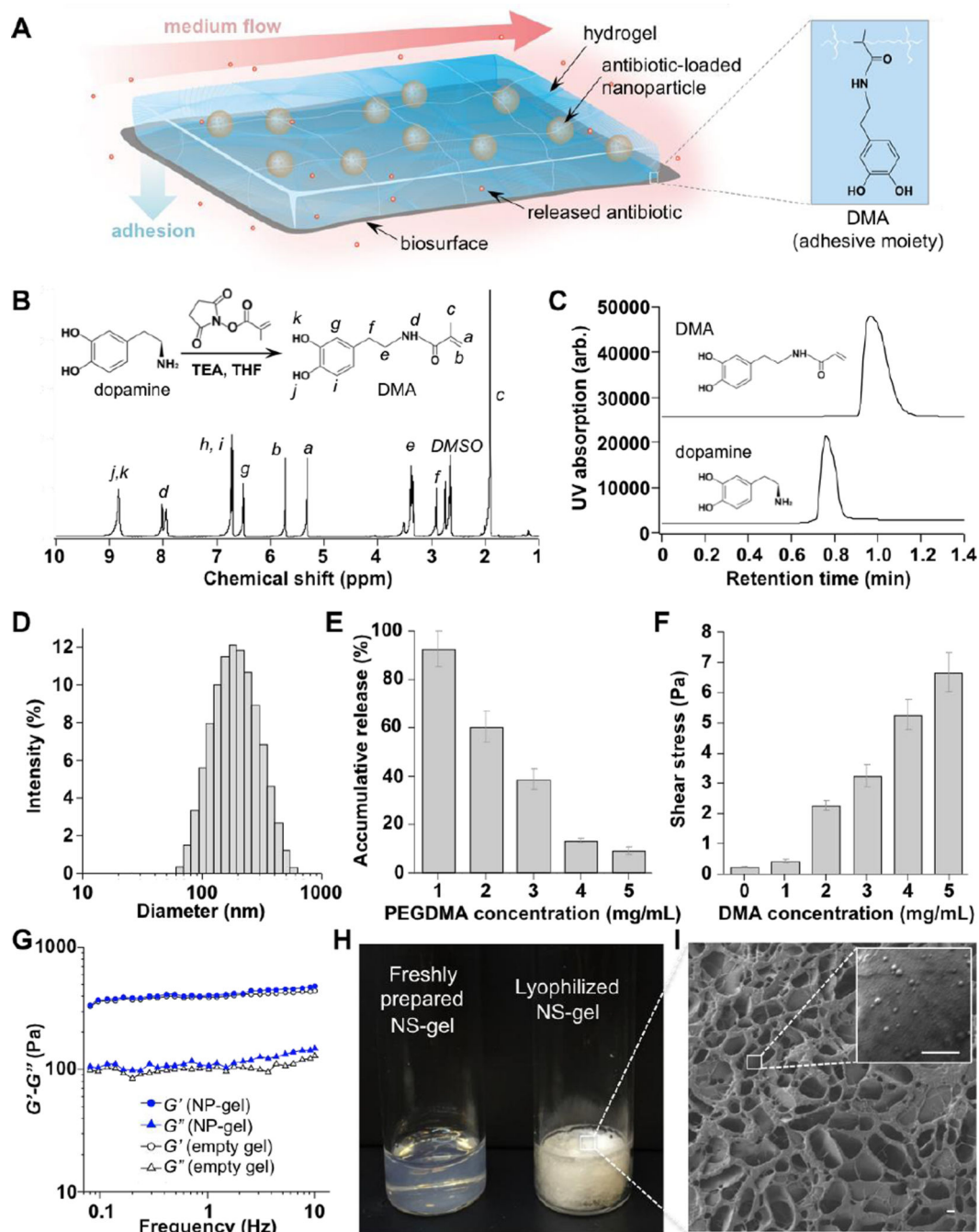


Figure 1. Formulation and characterization of tissue-adhesive nanoparticle-hydrogel hybrid (NP-gel) biomaterial system for controlled drug delivery. (A) Schematic illustration of such adhesive NP-gel system for localized antibiotic release to inhibit bacterial growth under flow conditions. In the formulation, dopamine methacrylamide (DMA) containing catechol functional group was used as an adhesive moiety. (B) Synthesis and $^1\text{H-NMR}$ spectrum of DMA. (C) Characteristic HPLC chromatograms of dopamine and DMA. (D) The hydrodynamic size (diameter, nm) of nanoparticles measured by dynamic light scattering

(DLS). (E) Accumulative release of nanoparticles from NP-gels with different poly(ethylene glycol) dimethacrylate (PEGDMA, cross-linker) concentrations when incubated at 37°C for 24 h. Error bars represent standard deviations (n = 3). (F) Shear stress of NP-gels with different DMA concentrations when detached from poly(vinyl alcohol) (PVA) membrane. (G) Rheological characterization of NP-gel (5 mg/mL PEGDMA and 5 mg/mL DMA) either loaded with 2 mg/mL nanoparticles (solid markers) or without nanoparticles (empty gel, open markers). (H) Photographs of freshly prepared NP-gel sample and lyophilized NP-gel sample. (I) A representative SEM image of the optimized NP-gel formulation. Scale bars, 1 μm .

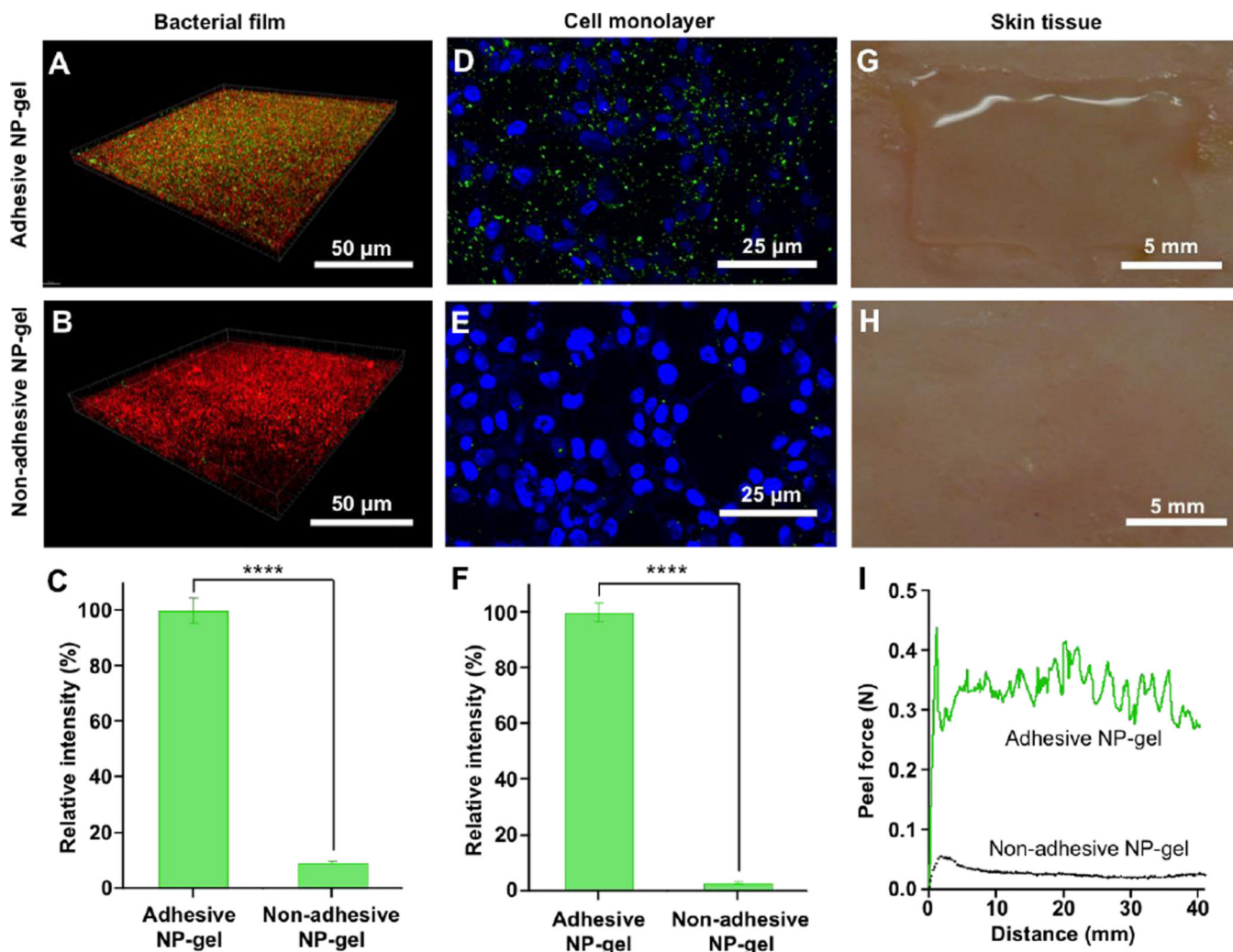


Figure 2.

Cell- and tissue-adhesive properties of the resulting NP-gel under flow conditions on various biological subjects, including: (A–C) *E. coli* bacterial film, (D–F) HEK 293T cell monolayer, and (G–I) shaved mouse skin tissue. In all studies, the shear stress from the flow of buffer solutions was kept constant at 3.2 Pa. Non-adhesive NP-gel (without addition of periodate) was used as a negative control. (A–B) *E. coli* bacteria were stained with propidium iodide (red) and nanoparticles embedded in the hydrogel were labeled with fluorescent dye DiO (green). (C) The fluorescence intensity of the nanoparticles retained on the bacterial film was quantified and compared. (D–E) HEK 293T cell monolayer was stained with DAPI (blue, nuclei) and nanoparticles embedded in the hydrogel were labeled with DiO (green). (F) The fluorescence intensity of the nanoparticles retained on the HEK 293T cell monolayer was quantified and compared. (G–H) Adhesive NP-gel remained attached to the mouse skin under flow condition, while non-adhesive control gel was washed away. (I) Plot of peel force and distance of adhesive and non-adhesive NP-gels on mouse skin when subjected to 180° peel loading. In G and F, data is shown as mean \pm SEM (**** p < 0.001).

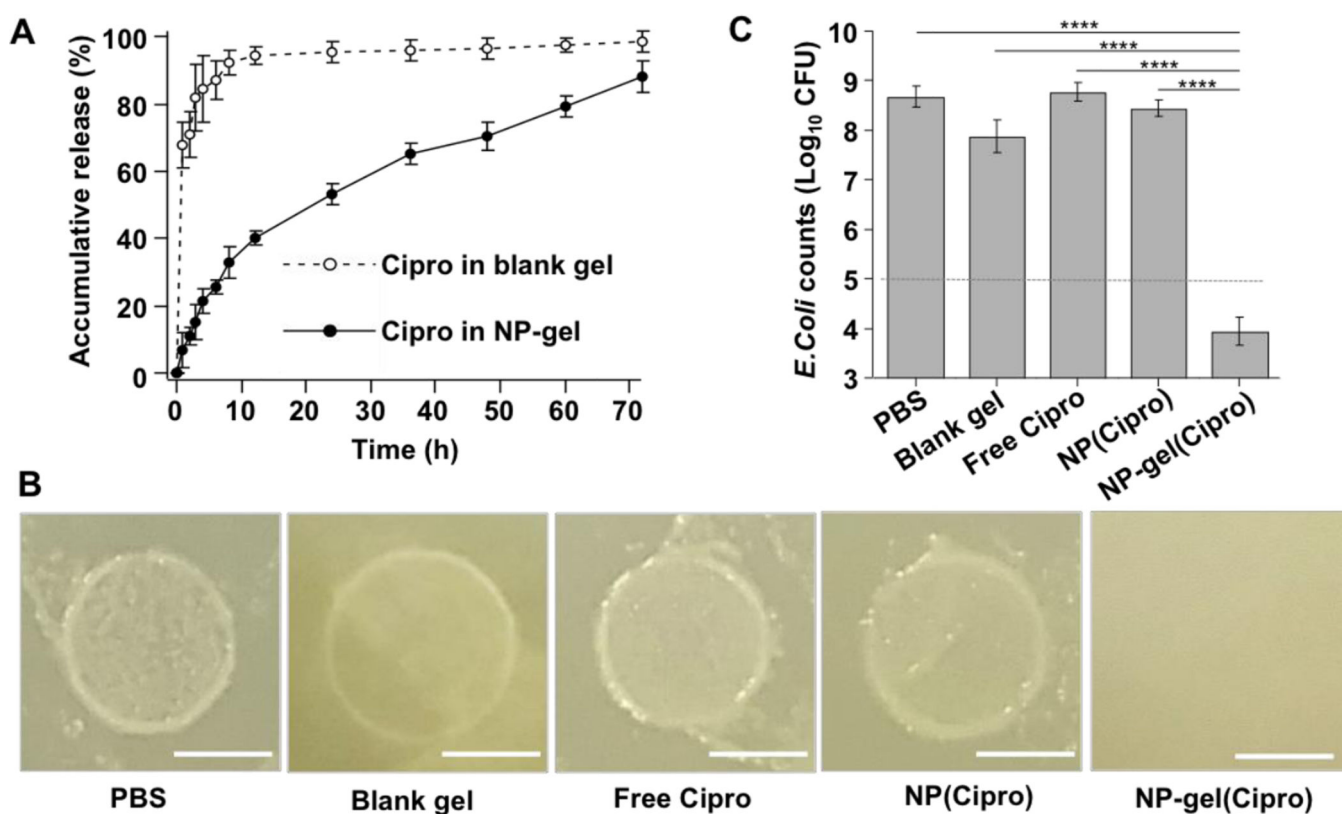


Figure 3.

Antimicrobial efficacy of antibiotic-loaded NP-gel against biofilm formation. (A) The accumulative release profile of ciprofloxacin (Cipro) from NP-gel, in which Cipro was loaded into the embedded nanoparticles. Free ciprofloxacin directly loaded in the corresponding hydrogel (blank gel without nanoparticles) was used as a control. (B) Photographs of *E. coli* biofilm formation with the treatment of PBS, blank gel (without nanoparticles or Cipro), free Cipro, Cipro-loaded nanoparticles (NP(Cipro), without hydrogel), and Cipro-loaded NP-gel (NP-gel(Cipro)). In the study, 5×10^6 CFU *E. coli* bacteria were inoculated to form and grow the biofilm. The medium buffer flow rate of all samples was kept at $10 \mu\text{L}/\text{min}$, corresponding to a dilution rate (flow rate divided by the volume of the well) of 0.005 min^{-1} . The images were taken 15 hrs post the initial bacterial inoculation. Scale bar = 5 mm. (C) Quantification of bacterial load of the biofilm samples in (B). Data is shown as mean \pm SEM (**** $p < 0.001$).

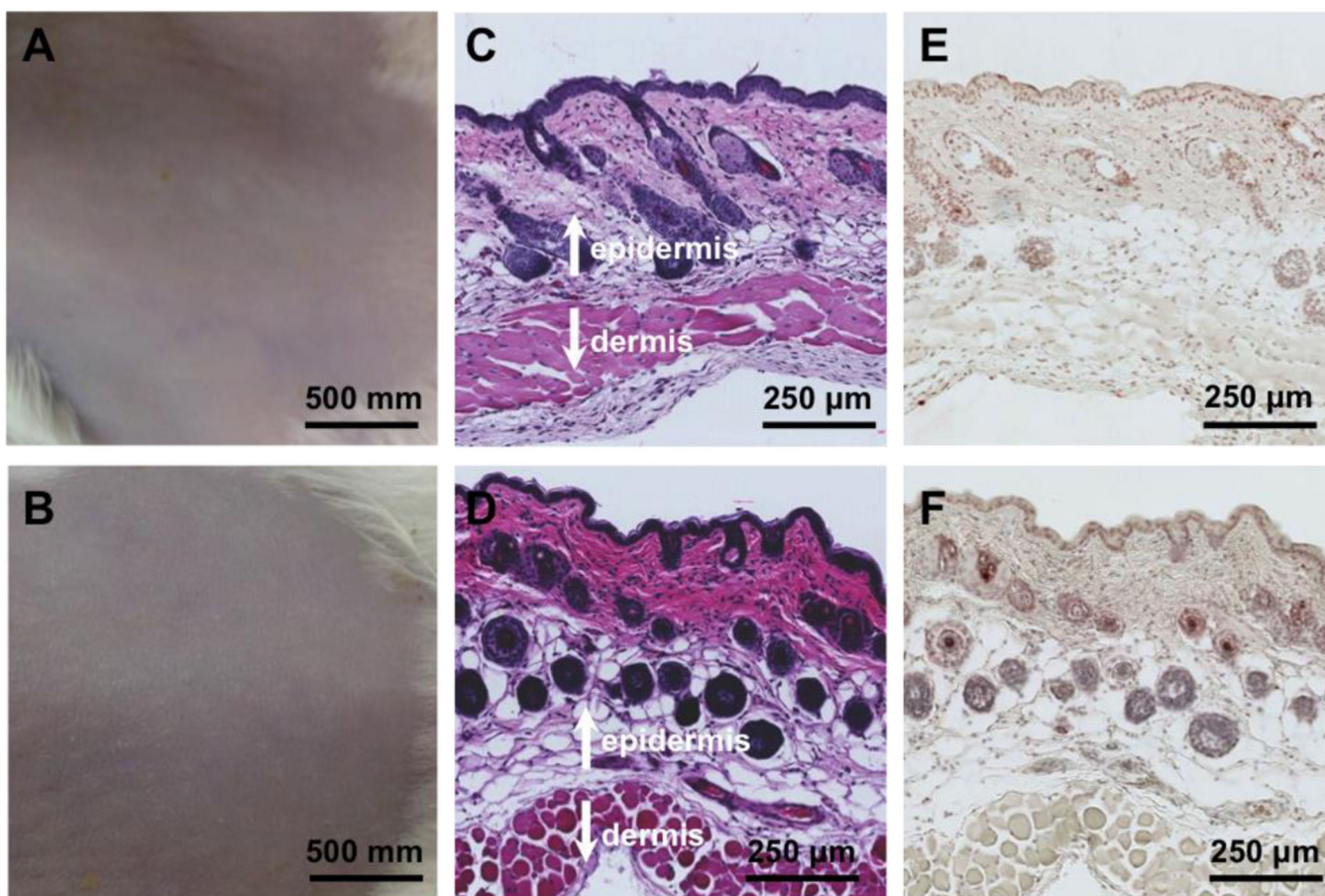


Figure 4. Toxicity evaluation of the NP-gel using a mouse skin model. Mouse skin was treated with PBS buffer (A, C, and E) and NP-gel (B, D, and F), respectively. The samples were applied onto the shaved skin once a day for 7 days. Following the last treatment, the skin morphology of the two treatment groups was examined (A and B). The skin sections were further examined after H&E staining (C and D) and TUNEL staining (E and F).